in Proc. IEEE SPAWC-2005, New York City, USA
June 2005, vol. I, pp. 648–652.

NONSTATIONARY VECTOR AR MODELING OF WIRELESS CHANNELS

*Michael Jachan and Gerald Matz**

Institute of Communications and Radio-Frequency Engineering, Vienna University of Technology
Gusshausstrasse 25/389, A-1040 Wien, Austria
phone: +43 1 58801 38914, fax: +43 1 58801 38999, email: michael.jachan@ieee.org

*On leave with Laboratoire des Signaux et Systèmes, Ecole Supérieure d'Electricité
3 Rue Joliot-Curie, F-91190 Gif-sur-Yvette, France

ABSTRACT

We propose a novel long-term parametric channel model for wireless channels that do not satisfy the usual assumption of wide-sense stationary uncorrelated scattering (WSSUS). Our non-WSSUS channel model is based on an innovations system representation that models the channel taps jointly as nonstationary vector autoregressive (AR) process, leading to a highly parsimonious description of the channel statistics. We also present a Yule-Walker type approach for estimating the parameters of this vector time-frequency AR model. Numerical results involving a simulated channel and real-world measurements illustrate the usefulness of our approach.

1. INTRODUCTION

Wireless channel models are indispensable for the design, simulation, and evaluation of wireless communication schemes. Preferably, these channel models should be simple enough to be analytically tractable and amenable for efficient numerical simulation while simultaneously reflecting real-world propagation effects in a realistic fashion. There are mainly two approaches to wireless channel modeling: geometry-based models and stochastic models.

Contributions. In this paper, we present a novel parametric approach for long-term stochastic channel modeling that is advantageous in terms of parsimony, flexibility, and generality. In essence, this paper extends the WSSUS channel model from [1] to non-WSSUS channels (cf. [2–4]) by using vector versions of the signal processing tools introduced in [5]. Specifically, after providing some background on non-WSSUS channels in Section 2, we use nonstationary vector autoregressive (AR) models, which we call vector time-frequency AR (VTFAR) models, to jointly describe the tap processes in a tapped delay line representation of the channel (Section 3). This allows to overcome the usual limitation to channels satisfying the assumption of *wide-sense stationary uncorrelated scattering* (WSSUS) [6, 7]. In Section 4 we furthermore propose an efficient Yule-Walker type approach for estimating the parameters involved in the VTFAR model. Simulation results for a synthetic single-tap channel and a measured real-world channel verify the usefulness of our ideas (Section 5).

Related Work. The characterization of non-WSSUS channels and nonparametric estimation of their statistics has been studied recently in [3, 4]. Scalar AR and ARMA models for the individual taps of WSSUS channels have been used for analysis and simulation purposes in [1, 8–11]. A multivariate AR model for stationary channels with correlated taps (i.e., no uncorrelated scattering) has been used for channel estimation and equalization [12].

Funding by FWF grant J2302 and by the European Community Network of Excellence NEWCOM (FP6-IST 507325).

2. NON-WSSUS CHANNELS

Tapped Delay Line. The starting point for our development is the representation of the wireless channel as a random time-varying linear system. Assuming a sampling rate (bandwidth) B and a block length of T samples, the discrete time channel input-output relation linking the transmit signal $s[t]$ and the receive signal $r[t]$ reads

$$r[t] = (\mathbb{H}\, s)[t] = \sum_{\tau=0}^{\tau_{\max}} \tilde{h}[t,\tau]\, s[t-\tau]\,. \qquad (1)$$

Here, $\tilde{h}[t,\tau]$ is the channel impulse response (which potentially incorporates transmit/receive filtering as well as antenna effects), τ denotes delay, and $\tau_{\max}$ is the maximum delay in samples (a maximum delay in seconds of τ_0 corresponds to $\tau_{\max} = \lceil \tau_0 B \rceil$). Eq. (1) corresponds to a tapped delay line model (cf. Fig. 1) with $\tau_{\max}+1$ taps that captures multipath (via the delays) as well as Doppler effects (via the time-dependence of $\tilde{h}[t,\tau]$). A more explicit characterization of the channel dispersion is provided by the *spreading function* $S_{\mathbb{H}}[\tau,\nu] = \mathop{\mathbb{F}}_{t\to\nu}\{\tilde{h}[t,\tau]\} \triangleq \sum_{t=0}^{T-1} \tilde{h}[t,\tau]\, e^{-j\frac{2\pi}{N}\nu t}$ (ν denotes discrete Doppler in samples), which allows to rewrite (1) as superposition of time-frequency shifts:

$$r[t] = \frac{1}{T} \sum_{\tau=0}^{\tau_{\max}} \sum_{\nu=-\nu_{\max}}^{\nu_{\max}} S_{\mathbb{H}}[\tau,\nu]\, s[t-\tau]\, e^{j\frac{2\pi}{N}\nu t}\,.$$

Here, $\nu_{\max}$ is the maximum Doppler in samples (related to the maximum Doppler ν_0 in Hz as $\nu_{\max} = \lceil \nu_0 T/B \rceil$).

Statistical Characterization. For WSSUS channels, $\tilde{h}[t,\tau]$ is a 2D random process that is stationary with respect to time t (WSS) and uncorrelated with respect to delay τ (US). In contrast, for non-WSSUS channels, the tap processes $\tilde{h}[t,\tau]$ are correlated nonstationary processes. The second-order statistics of a non-WSSUS channel $\mathbb{H}$ can be characterized via the 4D correlation function $R_{\tilde{h}}[t,\tau;\Delta t,\Delta\tau] \triangleq \mathcal{E}\{\tilde{h}[t,\tau+\Delta\tau]\tilde{h}^*[t-\Delta t,\tau]\}$. A physically more intuitive second-order statistics is the channel's time- and frequency-depending *local scattering function* (LSF) (cf. [2–4])

$$\mathcal{C}_{\mathbb{H}}[t,f;\tau,\nu] \triangleq \mathop{\mathbb{F}}_{\Delta t\to\nu} \mathop{\mathbb{F}^{-1}}_{\Delta\tau\to f} \{R_{\tilde{h}}[t,\tau;\Delta t,\Delta\tau]\}\,.$$

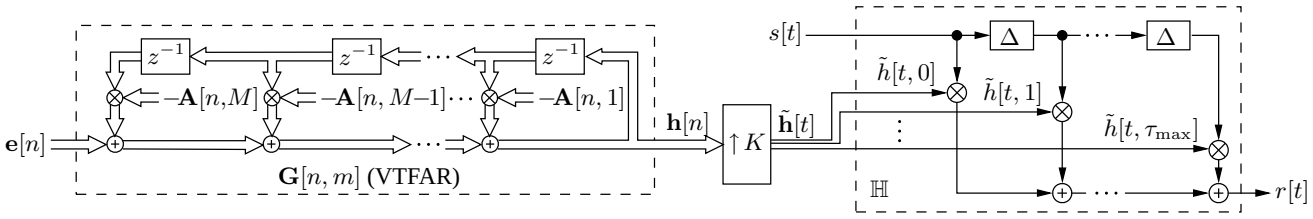

Figure 1: *The proposed non-WSSUS tapped delay line channel model (right part) including the VTFAR innovations representation of the tap processes (left part); z^{-1} and Δ are the unit delays with respect to the innovations rate and the system sampling rate, respectively.*

The LSF describes the mean power of scatterers causing a delay-Doppler shift by (τ,ν) at time t and frequency f. For WSSUS channels, the LSF reduces to the ordinary scattering function [6,7].

The *channel correlation function* (CCF) (cf. [2–4]), defined as

$$\mathcal{A}_{\mathbb{H}}[\Delta t,\Delta f;\Delta\tau,\Delta\nu] \stackrel{\triangle}{=} \mathop{\mathbb{F}}_{t\to\Delta\nu}\mathop{\mathbb{F}^{-1}}_{\tau\to\Delta f}\{R_{\tilde{h}}[t,\tau;\Delta t,\Delta\tau]\}\ ,$$

characterizes the correlation of scatterers separated by Δt, Δf, $\Delta\tau$, $\Delta\nu$ in time, frequency, delay, and Doppler.

3. PROPOSED CHANNEL MODEL

3.1. Innovations Representation

In this paper, we propose to base the modeling of the channel impulse response on a (vector) innovations representation, i.e., $\tilde{\mathbf{h}}[t] = [\tilde{h}[t,0]\dots\tilde{h}[t,\tau_{\max}]]^T$ is obtained by passing (temporally) white noise through a linear system with multiple inputs and multiple outputs. Since usually the time-variation (Doppler) of $\tilde{\mathbf{h}}[t]$ is much smaller than the sampling rate, we choose to split the innovations representation into a matrix innovations filter that operates at the "Doppler" innovations rate B/K and shapes the Doppler profile, followed by separate scalar interpolation stages for each tap with upsampling factor K satisfying $K \le B/\nu_0$ (cf. Fig. 1).

Since $\tilde{\mathbf{h}}[t]$ is nonstationary and has correlated entries, a time-varying matrix innovations filter is required to produce the subsampled channel impulse response $\mathbf{h}[n] = \tilde{\mathbf{h}}[nK]$, $n = 0,\dots,N-1$, according to

$$\mathbf{h}[n] = \sum_m \mathbf{G}[n,m]\,\mathbf{e}[n-m]\,. \tag{2}$$

Here, $\mathbf{G}[n,m]$ denotes the $(\tau_{\max}+1)\times(\tau_{\max}+1)$ causal time-varying matrix impulse response of the innovations filter and $\mathbf{e}[n]$ is a zero-mean innovations process with correlation $\mathcal{E}\{\mathbf{e}[n]\,\mathbf{e}^H[n']\} = \mathbf{\Sigma}[n]\,\delta[n-n']$. On first glance, nothing seems to be gained by using a time-varying matrix innovations filter to model a scalar time-varying channel; however, $\mathbf{G}[n,m]$ in (2) operates at the innovations rate which is much lower than the system rate (typically, $\log_{10} K = 3\dots5$). Furthermore, the matrix innovations filter $\mathbf{G}[n,m]$ is ideally suited for the parsimonious parametric VTFAR modeling approach presented in Section 3.2.

For WSSUS channels, it suffices to have separate time-invariant filters for each tap, i.e., in that case the innovations filter is diagonal and time-invariant, $\mathbf{G}[n,m] = \mathrm{diag}\{g_0[m],\dots,g_{\tau_{\max}}[m]\}$. In particular, $\mathbf{G}[n,m] = \mathbf{I}$ leads to a WSSUS channel with brick-shaped scattering function. We note that a time-invariant (but non-diagonal) matrix innovations filter has been previously used in [12], leading to a wide-sense stationarity channel model with correlated channel taps (i.e., WSS but non-US). A diagonal time-varying innovations filter $\mathbf{G}[n,m] = \mathrm{diag}\{g_0[n,m],\dots,g_{\tau_{\max}}[n,m]\}$ yields uncorrelated nonstationary tap processes (i.e., non-WSS but US). Finally, we note that a flat-fading (single tap) channel is obtained with a scalar innovations filter $g[n,m]$.

3.2. VTFAR Modeling

In this section, we propose to model the matrix innovations filter $\mathbf{G}[n,m]$ in the channel's innovations representation via a nonstationary VTFAR model. This is motivated by the specific usefulness of AR models to represent peaky Doppler profiles prevailing in practical situations. The fact that we choose a vector-valued and nonstationarity AR model is necessitated by our focus on non-WSSUS channels. These models can be viewed as vector extensions of the scalar time-frequency AR models in [5].

We will now represent the matrix innovations filter $\mathbf{G}[n,m]$ in terms of a VTFAR model. This amounts to specializing (2) as follows (cf. Fig. 1):

$$\sum_{m=0}^{M}\sum_{l=-L}^{L}\mathbf{A}_{m,l}\,\mathbf{h}[n-m]\,e^{j\frac{2\pi}{N}ln} = \mathbf{e}[n]\,. \tag{3}$$

Here, M and L denote the (temporal and spectral) model order, and $\mathbf{A}_{m,l}$ denotes the $(\tau_{\max}+1)\times(\tau_{\max}+1)$ VFTAR parameter matrices. Note that (3) augments stationary vector AR models by including additional frequency shifts. With the definition $\mathbf{A}[n,m] \stackrel{\triangle}{=} \sum_{l=-L}^{L}\mathbf{A}_{m,l}\,e^{j\frac{2\pi}{N}ln}$ we have alternatively

$$\sum_{m=0}^{M}\mathbf{A}[n,m]\,\mathbf{h}[n-m] = \mathbf{e}[n]\,,$$

which makes the model nonstationarity more obvious. We assume in the following that $\mathbf{A}_{0,l} = \mathbf{I}\,\delta[l]$ (i.e. $\mathbf{A}[n,0] = \mathbf{I}$). Furthermore, we assume that the VTFAR parameter matrices are banded, i.e., $A_{m,l}^{(\tau,\tau')} = 0$ for $|\tau-\tau'| > \Delta\tau_{\max}$ (the notation $A^{(\tau,\tau')}$ is used to denote the elements of a matrix $\mathbf{A}$). The bandedness of $\mathbf{A}_{m,l}$ is motivated by the fact that only neighboring channel taps will be correlated (for US channels $\Delta\tau_{\max} = 0$). Consequently, each VTFAR parameter matrix has $d \stackrel{\triangle}{=} (2\Delta\tau_{\max}+1)(\tau_{\max}+1) - \Delta\tau_{\max}(\Delta\tau_{\max}+1)$ non-zero elements on the $2\Delta\tau_{\max}+1$ main diagonals. Finally, we assume that that the noise correlation matrix $\mathbf{\Sigma}[n]$ has the same band-structure and temporal bandlimitation, i.e.,

$$\mathbf{\Sigma}[n] = \sum_{l=-L}^{L}\mathbf{\Sigma}_l\,e^{j\frac{2\pi}{N}ln} \tag{4}$$

and $\Sigma_l^{(\tau,\tau')} = 0$ for $|\tau-\tau'| > \Delta\tau_{\max}$.

The number of complex scalar parameters in our VTFAR channel equals $P = (M+1)(2L+1)d$, i.e., it grows linearly with M, L, $\Delta\tau_{\max}$ and $\tau_{\max}$. In practice, $\Delta\tau_{\max} = 1\dots2$ will be sufficient

to capture tap correlations. Furthermore, the temporal model order M, which characterizes the number of peaks in the Doppler spectrum per tap, will typically be less than ≈ 3. Finally, the spectral model order L is relevant for the amount of channel nonstationarity (i.e., variation of channel statistics), with reasonable values about ≈ 3. We conclude that the overall number of parameters P required to model the nonstationary channel statistics will typically be reasonably small.

4. VTFAR ESTIMATION

We next present an estimator for the VTFAR model parameters that presupposes the availability of a channel realization $\mathbf{h}[n]$ (obtained e.g. from a measurement campaign).

4.1. Estimation of $\mathbf{A}_{m,l}$

To estimate the VTFAR matrices $\mathbf{A}_{m,l}$, we propose a Yule-Walker type procedure. It is based on the recursion

$$\sum_{m=0}^{M}\sum_{l=-L}^{L}\mathbf{A}_{m,l}\,e^{j\frac{2\pi}{N}ln}\,\mathbf{R}_{\mathbf{h}}[n-m,m'-m]=\mathbf{R}_{\mathbf{e},\mathbf{h}}[n,m'] \quad (5)$$

for the channel correlation $\mathbf{R}_{\mathbf{h}}[n,m]\stackrel{\triangle}{=}\mathcal{E}\{\mathbf{h}[n]\,\mathbf{h}^H[n-m]\}$ (note that $R_{\mathbf{h}}^{(\tau,\tau')}[n,m]=R_{\tilde{h}}[Kn,\tau;Km,\tau-\tau']$) which is obtained by post-multiplying (3) with $\mathbf{h}^H[n-m']$, taking expectations on both sides, and using $\mathbf{R}_{\mathbf{e},\mathbf{h}}[n,m']\stackrel{\triangle}{=}\mathcal{E}\{\mathbf{e}[n]\,\mathbf{h}^H[n-m']\}$.Since $\mathbf{G}[n,m]$ is causal, the right-hand side of (5) vanishes for $m'>0$. Moving the first summand ($m=0$) in (5) to the righthand side and performing a Fourier transform $n\to l'$ then yields

$$\sum_{m=1}^{M}\sum_{l=-L}^{L}\mathbf{A}_{m,l}\,\mathbf{F}_{\mathbf{h}}[m'-m,\,l'-l]\,e^{j\frac{2\pi}{N}m(l-l')}=-\mathbf{F}_{\mathbf{h}}[m',l']\,, \quad (6)$$

which holds for $m'=1,2,\ldots,M$, and $l'=-L,-L+1,\ldots,L$. Here, $\mathbf{F}_{\mathbf{h}}[m',\,l']=\mathop{\mathbb{F}}_{n\to l'}\{\mathbf{R}_{\mathbf{h}}[n,m']\}$ is the expected matrix ambiguity function (EMAF) of the vector process $\mathbf{h}[n]$. For non-WSSUS channels that are correlation underspread [2,4], $\mathbf{F}_{\mathbf{h}}[m',\,l']$ vanishes for $(m',\,l')$ off the origin such that the phase factors in (6) can safely be approximated as $e^{j\frac{2\pi}{N}m(l-l')}\approx 1$. We then obtain

$$\sum_{m=1}^{M}\sum_{l=-L}^{L}\mathbf{A}_{m,l}\,\mathbf{F}_{\mathbf{h}}[m'-m,\,l'-l]=-\mathbf{F}_{\mathbf{h}}[m',\,l']\,, \quad (7)$$

which is a (block-)Toeplitz system of equations. In our case, these equations cannot be solved directly since we need to take into account the band structure of the $\mathbf{A}_{m,l}$. Hence, we write out the matrix-vector products in (7) explicitly and keep only the terms involving nonzero elements of $\mathbf{A}_{m,l}$:

$$\sum_{m=1}^{M}\sum_{l=-L}^{L}\sum_{\tau''\in\mathcal{T}(\tau)}A_{m,l}^{(\tau,\tau'')}\,F_{\mathbf{h}}^{(\tau'',\tau')}[m'-m,\,l'-l]=-F_{\mathbf{h}}^{(\tau,\tau')}[m',l']\,. \quad (8)$$

Here, $\mathcal{T}(\tau)=\{\max\{\tau-\Delta\tau_{\max},0\},\ldots,\min\{\tau+\Delta\tau_{\max},\tau_{\max}\}\}$. A suitable stacking of these equations with respect to τ', τ, l, and m (in that order) yields the equation

$$\mathcal{F}\mathbf{a}=-\mathbf{f} \quad (9)$$

(see the Appendix for details). Here, $\mathcal{F}$ is a $P'\times P'$ block Toeplitz matrix ($P'=M(2L+1)d$) containing the $F_{\mathbf{h}}^{(\tau,\tau')}[m',l']$, $\mathbf{f}$ is a length-P' vector with elements $F_{\mathbf{h}}^{(\tau,\tau')}[m',l']$, and $\mathbf{a}$ is a length-P' vector containing the VTFAR model parameters $A_{m,l}^{(\tau,\tau'')}$. Eq. (9) can be efficiently solved for $\mathbf{a}$ by exploiting the block Toeplitz structure. In practice, the EMAF $\mathbf{F}_{\mathbf{h}}[m,\,l]$ has to be replaced by the estimate

$$\hat{\mathbf{F}}_{\mathbf{h}}[m,l]=\sum_{n=m}^{N-1}\mathbf{h}[n]\mathbf{h}^H[n-m]\,e^{-j\frac{2\pi}{N}ln}$$

(note that for small $[m,l]$ this estimate features sufficient averaging to be statistically reliable), which leads to estimates $\hat{\mathcal{F}}$ and $\hat{\mathbf{f}}$ for the matrix $\mathcal{F}$ and the vector $\mathbf{f}$ in (9). The solution of (9) then equals

$$\hat{\mathbf{a}}=-\hat{\mathcal{F}}^{-1}\hat{\mathbf{f}}\,,$$

from which the VTFAR parameter estimates $\hat{\mathbf{A}}_{m,l}$ can be easily extracted.

4.2. Estimation of Noise Correlation

Since $\mathbf{R}_{\mathbf{e},\mathbf{h}}[n,0]=\mathbf{\Sigma}[n]$, the noise variance parameters $\mathbf{\Sigma}_l$ can be estimated based on the equation

$$\mathbf{\Sigma}[n]=\sum_{m=0}^{M}\sum_{l=-L}^{L}\mathbf{A}_{m,l}\,e^{j\frac{2\pi}{N}ln}\,\mathbf{R}_{\mathbf{h}}[n-m,-m]\,, \quad (10)$$

which is obtained by reconsidering (5) with $m'=0$. Passing to the EMAF domain via a DFT $n\to l'$, approximating phase factors with 1 (underspread property), and using the parametric representation (4) of $\mathbf{\Sigma}[n]$, we arrive at

$$\mathbf{\Sigma}_{l'}=\sum_{m=0}^{M}\sum_{l=-L}^{L}\mathbf{A}_{m,l}\,\mathbf{F}_{\mathbf{h}}[-m,\,l'-l]\,,\quad l'=-L,\ldots,L\,. \quad (11)$$

In practice, estimates $\hat{\mathbf{\Sigma}}_l$ are obtained from the equations (11) by replacing the VTFAR parameter matrices and the EMAF with their estimates $\hat{\mathbf{A}}_{m,l}$ and $\hat{\mathbf{F}}_{\mathbf{h}}[m,l]$. The resulting estimates, given by $\hat{\mathbf{\Sigma}}_{l'}=\sum_{m=0}^{M}\sum_{l=-L}^{L}\hat{\mathbf{A}}_{m,l}\,\hat{\mathbf{F}}_{\mathbf{h}}[-m,\,l'-l]$, $l'=-L,\ldots,L$, are not guaranteed, however, to have band structure and to correspond to positive semi-definite $\hat{\mathbf{\Sigma}}[n]$. These properties can be ensured by using *projections onto convex sets* (POCS) [13], i.e., by alternatingly projecting on the convex sets of banded matrices, positive semi-definite matrices, and matrices with band-limited entries.

5. SIMULATION RESULTS

5.1. Simulated Channel

We first consider an example taken from [3] with a narrowband flat fading mobile radio system ($B=98.304$kHz) at carrier frequency 2 GHz. For a duration of 10.67s, $1024^2=1048576$ channel samples are required. Assuming Doppler frequencies less than 50 Hz allows for $K=1024$ and $N=1024$.

The urban propagation scenario is a street crossing where a mobile performs a U-turn at constant speed. Two street canyons result in two main propagation paths with equal delay. Each path consists of S uncorrelated subpaths whose angular spread is $\delta=6^\circ$. The corresponding non-WSSUS channel $h[n,\tau]=h_0[n]\,\delta[\tau-\tau_0]$, $n=0,\ldots,1023$, was simulated according to

$$h_0[n]=\sum_{p=1}^{2}\sum_{s=1}^{S}\alpha_{p,s}\,e^{j\psi_{p,s}}\,\exp[j2\pi\,\nu_{\max}\cos(\phi_{p,s}[n])]\,,$$

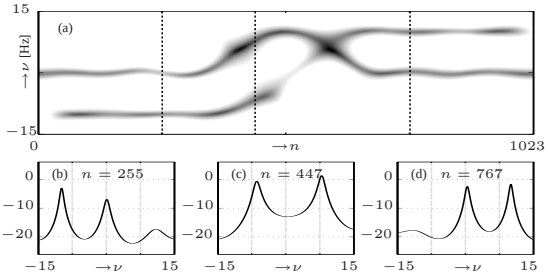

Figure 2: *TFAR based estimate ($M = L = 6$) of the time-varying Doppler profile $\mathcal{Q}[n, \nu]$ of the synthetic single-tap channel: (a) gray-scale plot, (b)–(d) slices at various time instants.*

where $\alpha_{p,s}$ and $\psi_{p,s}$ denote the random amplitude and phase of the sth subpath of the pth path. Furthermore, $\phi_{p,s}[n] = \bar{\phi}_p[n] + \Delta\phi_{p,s}$ is the angle of arrival (AOA), i.e., the angle between the directions of path propagation and mobile motion, of the sth subpath of the pth path, with $\bar{\phi}_p[n]$ the mean incidence angle associated to path #p and $\Delta\phi_{p,s} \in [-\frac{\delta}{2}, \frac{\delta}{2}]$ a uniformly distributed random angular "jitter." For fixed propagation paths, the angles $\bar{\phi}_1[n]$ and $\bar{\phi}_2[n]$ are determined by the motion of the mobile.

Since this channel consists of a single tap, the VTFAR model reduces to a scalar TFAR model ($\mathbf{\Sigma}[n] = \sigma^2[n]$, $\mathbf{A}_{m,l} = A_{m,l}$). The LSF of this channel is $\mathcal{C}_{\mathbb{H}}[n, f; \tau, \nu] = \mathcal{Q}[n; \nu]\, \delta[\tau - \tau_0]$ where $\mathcal{Q}[n, \nu]$ is the time-varying Doppler profile that can be approximated as $\mathcal{Q}[n, \nu] \approx \frac{\sigma^2[n]}{|\tilde{A}[n,\nu]|^2}$ with $\tilde{A}[n, \nu] = N \underset{m\to\nu}{\mathbb{F}} \underset{l\to n}{\mathbb{F}^{-1}}\{A_{m,l}\}$. Based on a single channel realization and using empirically determined model orders $M = L = 6$, we estimated the model parameters according to Section 4. The resulting estimated time-varying Doppler profile is shown in Fig. 2(a). It clearly reflects the different phases of the mobile movement with $\bar{\phi}_1[n] = 0$, $\bar{\phi}_2[n] = 90$ at the beginning (cf. Fig. 2(b)) and $\bar{\phi}_1[n] = 180$, $\bar{\phi}_2[n] = -90$ at the end (cf. Fig. 2(d)), whereas $\bar{\phi}_1[n] = -\bar{\phi}_2[n] = 45$ around $n = 440$ (cf. Fig. 2(c)). We note that this parametric estimate of $\mathcal{Q}[n, \nu]$ is very close to the nonparametric results in [3]. Furthermore, for a duration of more than 10 s, the channel statistics can be characterized by only $P = 91$ parameters as compared to 1024^2 values required in the nonparametric case.

5.2. Measured Channel

We next apply our ideas to a non-WSSUS channel that has been measured[1] within the framework of the METAMORP project (http://www.nt.tuwien.ac.at/mobile/projects/METAMORP). At a measurement bandwidth of $B = 10$ MHz and a carrier frequency of $f_c = 1792$ MHz, impulse response snapshots $h[n, \tau]$, $n = 1, \ldots, 2048$, $\tau = 1, \ldots, 64$, were recorded every 24.576 ms while the mobile receiver moved around a corner in a suburban propagation scenario, leading to a total measurement duration of 50.33 s (for further details, see [3]).

We applied our VTFAR modeling approach to the five dominant channel taps during a period of 12.6 s ($N = 512$) where the mobile passed the corner and turned right towards the base station. The pre-selected model orders were $\Delta\tau_{\max} = 1$, $M = 2$, and $L = 3$. It can be shown that a parametric estimate for the LSF of this channel can be obtained from the VTFAR parameter estimates according to

$$\hat{\mathcal{C}}_{\mathbb{H}}[n, f; \tau, \nu] = \frac{\hat{\sigma}^2[n, f; \tau]}{\left|\hat{a}[n, f; \tau, \nu]\right|^2}$$

with

$$\hat{\sigma}^2[n, f; \tau] = \underset{\Delta\tau\to f}{\mathbb{F}^{-1}} \left\{\hat{\Sigma}^{(\tau,\tau+\Delta\tau)}[n]\right\}$$

and

$$\hat{a}[n, f; \tau, \nu] = \underset{\Delta\tau\to f}{\mathbb{F}^{-1}} \underset{m\to\nu}{\mathbb{F}} \underset{l\to n}{\mathbb{F}^{-1}} \left\{\hat{A}_{m,l}^{(\tau,\tau+\Delta\tau)}\right\}$$

(due to lack of space, further details will be presented elsewhere). We observed that a slight regularization of the division in the above estimate results in improved performance. Six snapshots of the LSF estimate $\hat{\mathcal{C}}_{\mathbb{H}}[n, f; \tau, \nu]$ for $f = f_c$ and various time instants n are shown in Fig. 3 (normalized with the associated path loss $\hat{\rho}_{\mathbb{H}}[n, f_c] = \sum_\tau \sum_\nu \hat{\mathcal{C}}_{\mathbb{H}}[t, f_c; \tau, \nu]$). They clearly reflect the nonstationarity of the channel's statistics. Initially (Fig. 3(a)–(c)), while the base station is located broadside, significant multipath components with Doppler frequencies close to zero are present. After the mobile has turned right (Fig. 3(d)–(f)), the base station is located ahead of the mobile leading to a strong component about the maximum Doppler frequency of ≈ 10 Hz. A second, slightly weaker multipath component results from a building located behind the mobile. During the 12.6 s period, the path gain varies by about 5 dB. We finally emphasize that with our approach, $12.6\,s$ of channel statistics are fully characterized by only $P = 273$ scalar parameters (i.e., less than 5 parameters per tap per second).

6. CONCLUSIONS AND OUTLOOK

We presented a novel approach for long-term (i.e., several seconds) modeling of wireless channels that fail to satisfy the assumption of wide-sense stationary uncorrelated scattering (WSSUS). In the proposed channel model, the channel tap processes are obtained as output of an innovations system that operates at low rate followed by an interpolation stage. The innovations system itself is represented via a parsimonious vector time-frequency AR (VTFAR) model. We furthermore discussed a Yule-Walker type method for estimating the parameters of the VTFAR model.

Theoretical arguments and simulation results involving synthetic and measured channels demonstrated that our approach is useful to obtain physically intuitive characterizations of the channel statistics in terms of a small number of parameters. We note that the proposed model can also be used for efficient long-term simulation of non-WSSUS wireless channels based on prescribed VTFAR parameter sets.

Some open issues we are currently exploring are the selection of the model orders (M, L, $\Delta\tau_{\max}$) based on Akaike and minimum description length approaches as well as stabilization procedures for parameter estimates that do not correspond to stable models (cf. [14]). Finally, in practice the estimation of the channels expected matrix ambiguity function has to be modified to account for the fact that channel realizations cannot be directly observed.

A. DERIVATION OF (9)

Stacking (8) with respect to τ', $\tau'' \in \mathcal{T}(\tau)$ and using $\tau_{\min}(\tau) = \max\{\tau - \Delta\tau_{\max}, 0\}$, $\tau_{\max}(\tau) = \min\{\tau + \Delta\tau_{\max}, \tau_{\max}\}$, we obtain

$$\sum_{m,l} \mathbf{F}_{m'-m,l'-l,\,\tau}\, \mathbf{a}_{m,l,\tau} = -\mathbf{f}_{m',l',\tau}\,.$$

[1] Courtesy of T-NOVA Deutsche Telekom Innovationsgesellschaft mbH (Technologiezentrum Darmstadt, Germany). We are grateful to I. Gaspard and M. Steinbauer for providing us with the measurement data.

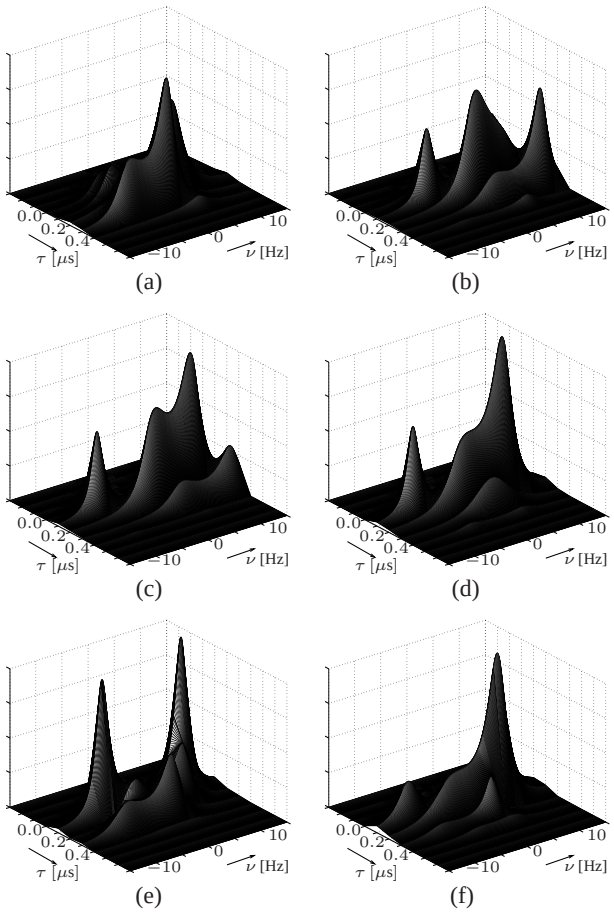

Figure 3: *Parametric LSF estimate* $\hat{\mathcal{C}}_{\mathbb{H}}[n, f_c; \tau, \nu]$ *obtained with* $\Delta\tau_{\max} = 1$, $M = 2$, $L = 3$ *at time instants (a)* $n = 864$, *(b)* $n = 928$, *(c)* $n = 992$, *(d)* $n = 1056$, *(e)* $n = 1120$, *(f)* $n = 1184$.

with the $|\mathcal{T}(\tau)| \times |\mathcal{T}(\tau)|$ block matrices

$$\mathbf{F}_{m,l,\tau} = \begin{bmatrix} F_{\mathbf{h}}^{(\tau_{\min}(\tau),\tau_{\min}(\tau))}[m,l] & \cdots & F_{\mathbf{h}}^{(\tau_{\max}(\tau),\tau_{\min}(\tau))}[m,l] \\ \vdots & & \vdots \\ F_{\mathbf{h}}^{(\tau_{\min}(\tau),\tau_{\max}(\tau))}[m,l] & \cdots & F_{\mathbf{h}}^{(\tau_{\max}(\tau),\tau_{\max}(\tau))}[m,l] \end{bmatrix},$$

and the $|\mathcal{T}(\tau)| \times 1$ vectors

$$\mathbf{f}_{m,l,\tau} = \begin{bmatrix} F_{\mathbf{h}}^{(\tau,\tau_{\min}(\tau))}[m,l] & \cdots & F_{\mathbf{h}}^{(\tau,\tau_{\max}(\tau))}[m,l] \end{bmatrix}^T,$$
$$\mathbf{a}_{m,l,\tau} = \begin{bmatrix} a_{m,l}^{(\tau,\tau_{\min}(\tau))} & \cdots & a_{m,l}^{(\tau,\tau_{\max}(\tau))} \end{bmatrix}^T.$$

We next arrange the $\mathbf{F}_{m,l,\tau}$ into $d \times d$ block-diagonal matrices

$$\mathbf{F}_{m,l} = \operatorname{diag}\{\mathbf{F}_{m,l,\tau}\}_{\tau=0}^{\tau_{\max}},$$

and correspondingly build the $d \times 1$ vectors

$$\mathbf{f}_{m,l} = \begin{bmatrix} \mathbf{f}_{m,l,0}^T & \cdots & \mathbf{f}_{m,l,\tau_{\max}}^T \end{bmatrix}^T,$$
$$\mathbf{a}_{m,l} = \begin{bmatrix} \mathbf{a}_{m,l,0}^T & \cdots & \mathbf{a}_{m,l,\tau_{\max}}^T \end{bmatrix}^T.$$

These quantities are next stacked with respect to l, to obtain the $(2L+1)d \times (2L+1)d$ block-Toeplitz matrices[2]

$$\mathbf{F}_m = \operatorname{toep}\{\mathbf{F}_{m,-2L}, \cdots, \mathbf{F}_{m,2L}\},$$

[2]The notation $\operatorname{toep}\{\cdot\}$ is used to denote block-Toeplitz matrices whose block-diagonal elements are the matrices specified as arguments.

and the $(2L+1)d \times 1$ vectors $\mathbf{f}_m = \begin{bmatrix} \mathbf{f}_{m,l}^T & \cdots & \mathbf{f}_{m,l}^T \end{bmatrix}^T$ and $\mathbf{a}_m = \begin{bmatrix} \mathbf{a}_{m,-L}^T & \cdots & \mathbf{a}_{m,L}^T \end{bmatrix}^T$. Finally, a stacking with respect to m yields the $M(2L+1)d \times M(2L+1)d$ matrix

$$\mathcal{F} = \operatorname{toep}\{\mathbf{F}_{1-M}, \cdots, \mathbf{F}_{M-1}\}$$

and the $M(2L+1) \times 1$ vectors $\mathbf{f} = \begin{bmatrix} \mathbf{f}_1{}^T & \cdots & \mathbf{f}_M{}^T \end{bmatrix}^T$, $\mathbf{a} = \begin{bmatrix} \mathbf{a}_1{}^T & \cdots & \mathbf{a}_M{}^T \end{bmatrix}^T$. It is straightforward (although tedious) to show that with these definitions (8) is indeed equivalent to (9).

REFERENCES

[1] D. Schafhuber, G. Matz, and F. Hlawatsch, "Simulation of wideband mobile radio channels using subsampled ARMA models and multistage interpolation," in *Proc. 11th IEEE Workshop on Statistical Signal Processing*, (Singapore), pp. 571–574, Aug. 2001.

[2] G. Matz, "On non-WSSUS wireless fading channels," *IEEE Trans. Wireless Comm.*, Nov. 2005.

[3] G. Matz, "Characterization of non-WSSUS fading dispersive channels," in *Proc. IEEE ICC-2003*, (Anchorage, AK), pp. 2480–2484, May 2003.

[4] G. Matz, "Doubly underspread non-WSSUS channels: Analysis and estimation of channel statistics," in *Proc. IEEE SPAWC-03*, (Rome, Italy), pp. 190–194, June 2003.

[5] M. Jachan, G. Matz, and F. Hlawatsch, "Time-frequency-autoregressive random processes: Modeling and fast parameter estimation," in *Proc. IEEE ICASSP-2003*, vol. VI, (Hong Kong), pp. 125–128, April 2003.

[6] P. A. Bello, "Characterization of randomly time-variant linear channels," *IEEE Trans. Comm. Syst.*, vol. 11, pp. 360–393, 1963.

[7] J. G. Proakis, *Digital Communications*. New York: McGraw-Hill, 3rd ed., 1995.

[8] M. K. Tsatsanis and Z. D. Xu, "Pilot symbol assisted modulation in frequency selective fading wireless channels," *IEEE Trans. Signal Processing*, vol. 48, pp. 2353–2365, Aug. 2000.

[9] K. E. Baddour and N. C. Beaulieu, "Autoregressive models for fading channel simulation," in *Proc. IEEE GLOBECOM-2001*, (San Antonio, TX), pp. 1187–1192, Nov. 2001.

[10] S. M. Kay and S. B. Doyle, "Rapid estimation of the range-Doppler scattering function," *IEEE Trans. Signal Processing*, vol. 51, pp. 255–268, Jan. 2003.

[11] R. A. Ziegler and J. M. Cioffi, "Estimation of time-varying digital radio channels," *IEEE Trans. Veh. Technol.*, vol. 41, pp. 134–151, May 1992.

[12] M. K. Tsatsanis, G. B. Giannakis, and G. Zhou, "Estimation and equalization of fading channels with random coefficients," *Signal Processing*, vol. 53, pp. 211–229, Sept. 1996.

[13] P. L. Combettes, "The foundations of set theoretic estimation," *Proc. IEEE*, vol. 81, pp. 181–208, Feb. 1993.

[14] M. Jachan, G. Matz, and F. Hlawatsch, "TFARMA models: Order estimation and stabilization," in *Proc. IEEE ICASSP-2005*, (Philadelphia, PA), pp. 301–304, March 2005.